



Research article

A study on the surface grinding process of the SUJ2 steel using CBN slotted grinding wheel

Nhu-Tung Nguyen and Do Duc Trung*

Faculty of Mechanical Engineering, Hanoi University of Industry, Hanoi City, 100000, Vietnam

* **Correspondence:** Email: doductrung@hau.edu.vn; Tel: +84988488691; Fax: +842437655261.

Abstract: Using slotted grinding wheel in machining is a new approach in grinding technology. The slotted grinding wheel is used to improve the introduction of cool lubricant into the cutting zone, improve chip release condition and heat release condition during machining, thereby facilitating to improve the efficiency of the grinding process. However, up to now, the studies that are performed using this type of grinding wheel is very limited. To contribute some results to this rather new research direction, in this article we present the grinding process of SUJ2 steel using CBN slotted grinding wheel. The orthogonal Taguchi matrix with nine experiments was used to design the experimental matrix with three input parameters including workpiece velocity, feed rate, and depth of cut. The output parameters that were used to evaluate the quality and effectiveness of the grinding process were surface roughness, system vibrations in X, Y, Z directions, and the material removal rate. In surface grinding process using CBN slotted grinding wheel, all three input parameters (workpiece velocity, feed rate, and depth of cut) have a significant influence on the surface roughness, vibration. In which, the feed rate has the most influence on the output parameters. The second factor that influenced on the output parameter was the depth of cut. The workpiece velocity has the smallest influence on the output parameters. Data Envelopment Analysis Based Ranking (DEAR) method was used to solve the multi-objective optimization problem in surface grinding process. By applying this method, the optimal value of input parameter that were determined to obtain the minimum values of surface roughness and system vibration components, and to obtain the maximum of material removal rate. The optimum values of input parameters were the workpiece velocity of 15 m/min, the feed rate of 4 mm/stroke, and cutting depth of 0.015 mm. DEAR method can be applied to improve the quality and the effectiveness of the grinding process by reducing the surface roughness and system vibration components and increasing the material removal rate.

Keywords: CBN slotted grinding wheel; SUJ2 steel; surface roughness; vibration; MRR; DEAR

1. Introduction

Grinding processes are the most common method for machining surfaces that require high precision and surface gloss [1–3]. Surface roughness when grinding has a great influence on the workability and life of the parts. Therefore, surface roughness is often chosen to evaluate the efficiency of grinding processes in general and surface grinding in particular [4–7]. The vibrations of the grinding machine spindle, even with small amplitudes have a significant effect on the cutting depth of the grinding grain on the machining surface, too. Thereby the vibrations influence on the grinding productivity, surface quality. And the also influence on the irregular wear of grinding wheel [8–11]. Therefore, research to find solutions to reduce the vibrations of the grinder spindle also needs to be carried out under the specific machining conditions. The vibrations of the grinder spindle consist of forced vibration and self-vibration [12].

The forced vibration is transmitted by external factors. Factors causing the forced vibration can be mentioned as grinding wheel imbalance, bearing error, assembly error [13]. Self-vibrating is vibration that occurs during grinding, which is highly dependent on the uniformity of the workpiece material, cutting conditions, and grinding wheel properties [9,10]. Compared with forced vibration, the reduction of self- vibrations is much more advantages, this can be accomplished by changing some of the factors that influence on vibrations such as selecting the suitable cutting conditions [9,14]. However, the cutting conditions ensure that the vibration component in one direction has a small value, it does not guarantee that the vibration components in other directions and the surface roughness are also small. To determine the set of values of the cutting conditions with minimum of all vibration components and surface roughness, the multi-objective optimization process should be performed in each specific case [15].

Studies to improve the quality and productivity of grinding have been carried out by many authors. In grinding technology, two research directions that were focused to perform were grinding the new materials such as YAG single crystals [16], GGG single crystals [17], etc. and grinding by new grinding wheels. The study on using a grinding wheel with an interrupted working surface (including segmented grinding wheel and slotted grinding wheel) is also one of the research directions that has been focused by some scientists. Using slotted wheel can reduce cutting heat by 40% to 80% compared with conventional grinding wheels [18]. Using segmented wheel stones can reduce the cutting force by up to 30% compared with conventional grinding wheels [19]. Both surface roughness and cutting force when using segmented wheels have a smaller value than when using conventional grinding wheel [20,21]. Some recommendations when using a slotted aluminum oxide grinding wheel have also been proposed: surface roughness will have a minimum value when the number of grooves in the stone 18 (grooves) [22], cutting force is minimized when the grooves in the grinding wheel are 20 grooves [23]. However, only aluminum oxide grinding wheels (segmented and slotted types) were in these studies. CBN grinding wheel has the machining ability with small surface roughness and higher productivity than conventional grinding wheels with good cutting ability and high thermal resistance [24–26]. This grinding wheel could be applied to grind the surface with high accuracy and with small value of surface roughness due to its ability to maintain the sharpness of the grinding grains for a long time. Besides, this grinding wheel can also be used under

the dry grinding condition, which is almost impossible with aluminum oxide grinding wheels.

SUJ2 steel is a type of steel that is very popularly used to make machine parts with tensile loading such as shaft, gears, machine parts after forging, piston shaft, rolling shaft, mold (guide shaft, mold housing, ect). Grinding is often chosen as the final machining method of this steel when machining parts requiring high precision. However, it seems that, up to now, there have not been any studies using the CBN slotted grinding wheel. And more specifically, it has not seen any research using CBN slotted grinding wheel when grinding SUJ2 steel to determine the optimal value of cutting parameters to ensure the smallest surface roughness, the smallest vibration components, and largest material removal rate (MRR). These are the reasons for this study.

2. Experimental method using CBN slotted grinding wheel

2.1. Experimental workpiece

Workpiece in this work is SUJ2 steel which had heat treated to archive 62HRC in hardness. The compositions of SUJ2 steel are listed in Table 1. The properties of the of SUJ2 steel are listed in Table 2 (Equivalent to 100Cr6 steel according to DIN standard). The length, width, and height of workpieces were 60, 40 and 10 mm, respectively.

Table 1. Composition of SUJ2 steel [27].

Element	C	Si	Mn	Cr	Al	Cu
%	1.00	0.25	0.35	1.45	0.02	0.1

Table 2. Properties of SUJ2 steel [28].

Quantity	Value	Unit
Youngs module	210	GPa
Poisson's ratio	0.3	-
Shear module	80	GPa
Density	7800	kg/m ³
Average CTE 20–300 °C	12	μm/m°K
Specific heat capacity 50/100 °C	460–480	J/kg°K
Thermal conductivity ambient temperature	40–45	W/m°K
Electrical resistivity ambient temperature	0.20–0.25	μΩm

2.2. Experimental machine and grinding wheel

The surface grinding machine (APSG-820/2A, Taiwan) was used to perform the experiments. The CBN grinding wheel was used with the sign of HY-180x13x31.75-100# (Korea). The external diameter, thickness, and hole diameter of grinding wheels were 180, 31.75 and 13 mm, respectively. In the cylinder surface of grinding wheel, a groove was created with the depth of 2 mm and the width of 3 mm as shown in Figure 1.



Figure 1. CBN slotted grinding wheel.

2.3. Measurement system

The surface roughness of the machined parts was measured by MITUTOYO-Surface tester SJ-210 surface roughness tester. The evaluation length was fixed at 3×0.8 mm (three times of the standard length). The surface roughness was measured perpendicular to the cutting velocity direction and repeated three times following three repeated times of each cutting test. The surface roughness that was used for analysis and evaluation was the average value of surface roughness of three measurement consecutive times.

The measurement system including the acceleration sensor Type 4525-B-001, the data processing box, and the PULSE software was used to measure the system vibrations. For each experiment, the system vibrations were measured simultaneously in three directions (X, Y, Z). The detail is illustrated in Figure 2.

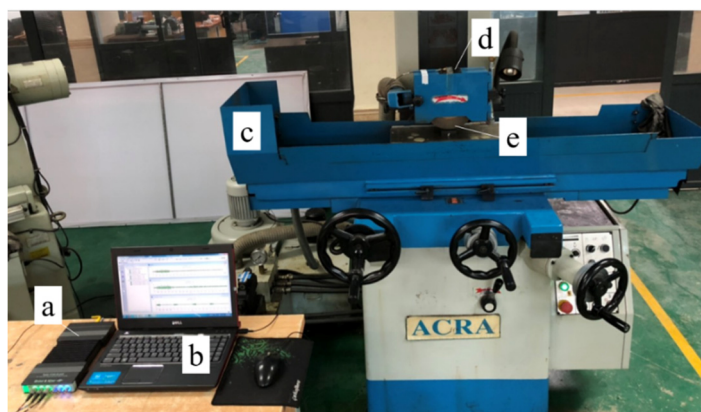


Figure 2. Measurement system of vibrations. (a) Data processing box; (b) PC and software; (c) grinding machine; (d) acceleration sensor; (e) grinding wheel.

The material removal rate (MRR) was calculated by Eq 1 [9,10].

$$MRR = V \times t \times b \text{ (mm}^3\text{/s)} \quad (1)$$

where: V is the workpiece velocity (mm/s); t is the depth of cut (mm); b is the width of cut (mm).

In this study, the width of the grinding wheel is 13 mm, the width of the groove in the cylinder surface of grinding wheel is 2 mm, so the width of cut is 11 mm.

2.4. Design of experimental matrix

In this study, the Taguchi method was used to design the experimental matrix. Three factors that were the workpiece velocity (V), feed rate (f), and depth of cut (t) were selected as the controllable factors. These are the parameters that the engineer can easily control when operating the machining machine. The levels of these parameters were expressed in Table 3. In the experimental layout plan, the most suitable orthogonal array (L₉) was selected to design the experimental matrix as listed in Table 4.

Table 3. Input parameters and their levels.

Parameters	Unit	Symbol	Actual value at the level		
			1	2	3
Workpiece velocity	m/min	V	5	10	15
Feed rate	mm/stroke	f	2	3	4
Depth of cut	mm	t	0.01	0.015	0.02

Table 4. Experimental matrix.

No.	Coded value			Actual value		
	V	f	t	V (m/min)	f (mm/stroke)	t (mm)
1	1	1	1	5	2	0.01
2	1	2	2	5	3	0.015
3	1	3	3	5	4	0.02
4	2	1	2	10	2	0.015
5	2	2	3	10	3	0.02
6	2	3	1	10	4	0.01
7	3	1	3	15	2	0.02
8	3	2	1	15	3	0.01
9	3	3	2	15	4	0.015

2.5. Experimental conditions

The experiments were conducted with the controllable factors in Table 5 and with the grinding conditions as following:

- Grinding wheel velocity: 26 m/s.
- Dressing conditions: dressing depth 0.01 (mm), dressing feed rate: 100 (mm/min).
- Cooling fluid: emulsion 10%, overflow irrigation method, volume flow rate of 4.6 lit/min.

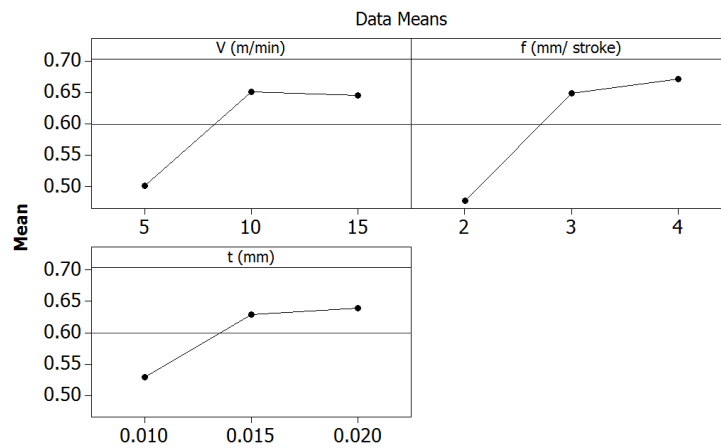
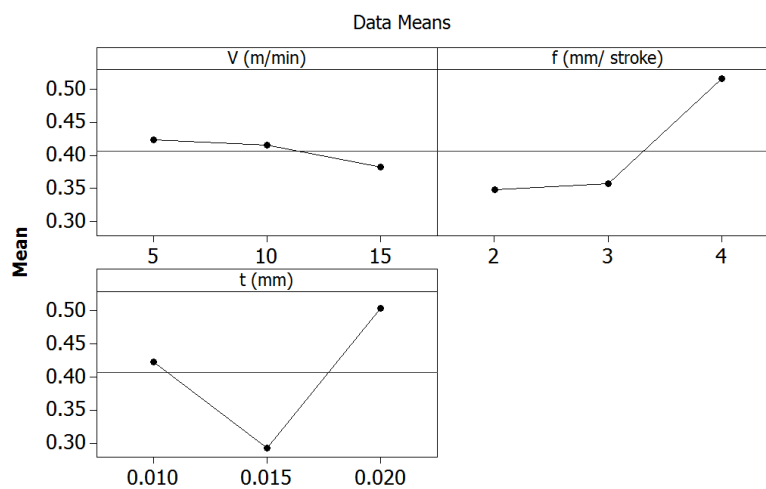
3. Experimental results and discussions

The experimental results of surface roughness, system vibrations in X, Y, Z directions, and MRR at each experiment were listed in Table 5.

Table 5. The experimental results.

No.	V (m/min)	f (mm/stroke)	t (mm)	Ra (μm)	Ax (μm)	Ay (μm)	Az (μm)	MRR (mm^3/s)
1	5	2	0.01	0.281	0.3683	0.5687	0.3419	9.1667
2	5	3	0.015	0.609	0.2632	0.3177	0.2216	13.7500
3	5	4	0.02	0.613	0.6379	0.7686	0.5712	18.3333
4	10	2	0.015	0.558	0.2491	0.2740	0.2791	27.5000
5	10	3	0.02	0.713	0.4502	0.5652	0.4541	36.6667
6	10	4	0.01	0.683	0.5450	0.6599	0.6358	18.3333
7	15	2	0.02	0.592	0.4249	0.4157	0.4068	55.0000
8	15	3	0.01	0.624	0.3573	0.3684	0.3392	27.5000
9	15	4	0.015	0.720	0.3641	0.4018	0.4123	41.2500

From the experimental results in Table 5, the influence degree of input parameters on the surface roughness and system vibration components in three directions X, Y, Z were investigated and shown from Figures 3–6.

**Figure 3.** Main effects plot for Ra.**Figure 4.** Main effects plot for Ax.

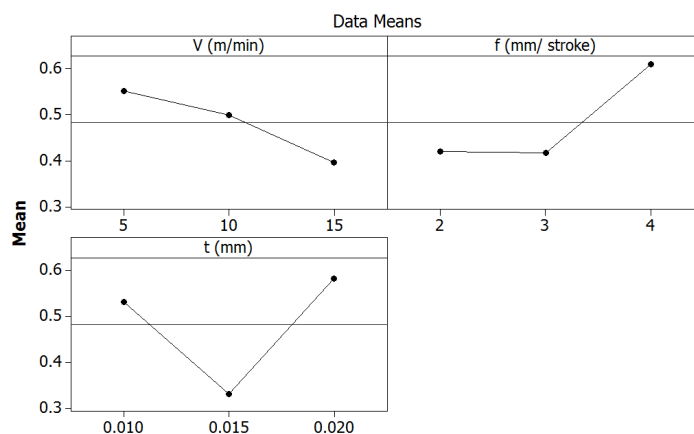


Figure 5. Main effects plot for Ay.

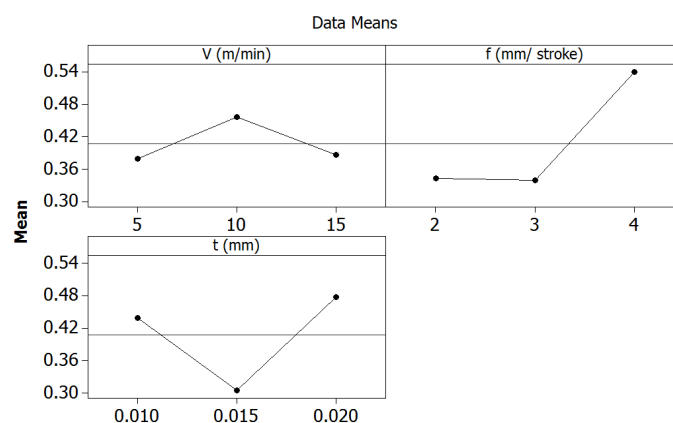


Figure 6. Main effects plot for Az.

The results were analyzed as following:

-The feed rate has the most influence on the machining surface roughness. The second factor that influenced on the machining surface roughness was the workpiece velocity. The depth of cut has the smallest influence on the surface roughness.

-When the workpiece velocity increases from 5 to 10 m/min, the surface roughness increases quickly. However, when the workpiece velocity increases from 10 to 15 m/min, the surface roughness decreases slowly. When increasing the feed rate from 2 to 3 mm/stroke, the surface roughness increases quickly. When increasing the feed rate from 3 to 4 mm/stroke, the surface roughness also increases, but it increases slowly. The influence of depth of cut on the surface is the same the influence of the feed rate on the surface roughness. When increasing the depth of cut from 0.01 to 0.015 mm, the surface roughness increases quickly. When increasing the depth of cut from 0.015 to 0.02 mm, the surface roughness also increases, but it increases slowly.

-The feed rate has the most influence on the vibration amplitude in X direction (Ax). The second factor that influenced on the Ax was the depth of cut. The workpiece velocity has a negligible effect on the Ax.

-When the feed rate increases from 2 to 3 mm/stroke, Ax increases slowly. However, when increasing the feed rate from 3 to 4 mm/stroke, Ax increases quickly. When increasing the depth of

cut from 0.01 to 0.015 mm, A_x decreases quickly. But, when increasing the depth of cut from 0.015 to 0.02 mm, A_x increases quickly.

-The feed rate has also the most influence on the vibration amplitude in Y direction (A_y). The second factor that influenced on the A_y was the workpiece velocity. The depth of cut has a negligible effect on the A_y .

-When the workpiece velocity increases, A_y decreases. When the feed rate increases from 2 to 3 mm/stroke, the feed rate almost has not influence on A_y . However, when increasing the feed rate from 3 to 4 mm/stroke, A_y increases quickly.

-The feed rate has also the most influence on the vibration amplitude in Z direction (A_z). When the feed rate increases from 2 to 3 mm/stroke, the feed rate has a negligible effect on the A_z . However, when increasing the feed rate from 3 to 4 mm/stroke, this parameter has large influence on A_z . The workpiece velocity and depth of cut have a negligible effect on the A_z .

The interaction influence of input parameters on the output parameters were described from Figures 7–10. The results from these figures showed that the input parameters have the complex interaction influence on the evaluation criteria.

Figure 7 describes the interaction influence of input parameters on the surface roughness, the results from this figure showed that:

-In the case the workpiece velocity was 5 m/min: When the feed rate increases from 2 to 3 mm/stroke, the surface roughness increases quickly. However, if the feed rate continues increasing, the surface roughness changes very small.

-In the case the workpiece velocity was 10 m/min: When the feed rate increases from 2 mm/stroke to 3 mm/stroke, the surface roughness increases. However, if the feed rate continues increasing, the surface roughness decreases.

-In the case the workpiece velocity was 15 m/min: When the feed rate increases, the surface roughness increases slowly.

-In the case the workpiece velocity was 5 m/min: When the depth of cut increases from 0.01 to 0.015 mm, the surface roughness increases quickly. But, if the depth of cut continues increasing, the surface roughness almost does not change.

-In the case the workpiece velocity was 10 m/min: When the depth of cut increases from 0.01 to 0.015 mm, the surface roughness decreases. But, if the depth of cut continues increasing, the surface roughness increases.

-In the case the workpiece velocity was 15 m/min: When the depth of cut increases from 0.01 to 0.015 mm, the surface roughness increases. But, if the depth of cut continues increasing, the surface roughness decreases.

-In the case the feed rate was 2 mm/stroke: If the depth of cut increases from 0.01 to 0.015 mm, the surface roughness increases quickly. But, if the depth of cut continues increasing, the surface roughness increases slowly.

-In the case the feed rate was 3 mm/stroke: The surface roughness decreases slowly if the depth of cut increases from 0.01 to 0.015 mm. However, if the depth of cut increases from 0.015 to 0.02 mm, the surface roughness increases quickly.

-In the case the feed rate was 4 mm/stroke: The surface roughness increases slowly if the depth of cut increases from 0.01 to 0.015 mm. However, if the depth of cut continues increasing, the surface roughness decreases quickly.

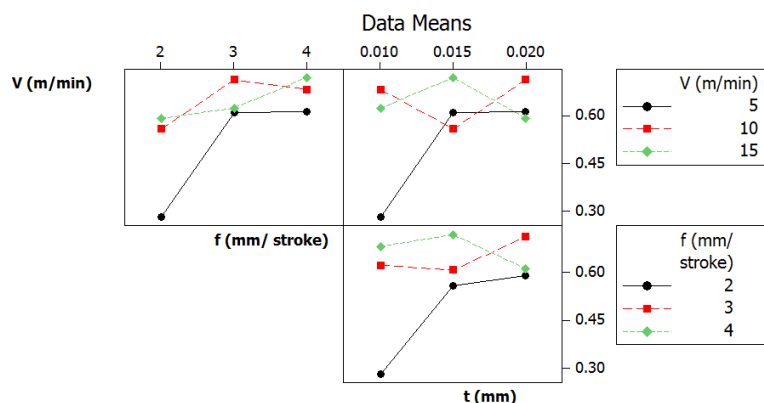


Figure 7. Interaction plot for Ra.

The interaction influence of input parameters on the system vibration amplitude in x direction (A_x) was described in Figure 8, the results from this figure showed that:

-In the case the workpiece velocity was 5 m/min: A_x decreases if the feed rate increases from 2 to 3 mm/stroke. But if the feed rate continues increasing, A_x increases quickly.

-In the case the workpiece velocity was 10 m/min, if the feed rate increases, A_x will increase. While, in the case the workpiece velocity was 15 m/min, if the feed rate increases from 2 to 3 mm/stroke, A_x will decrease, and if the feed rate increases from 3 to 4 mm/stroke, A_x almost does not change.

-In both cases of the workpiece velocity (5 and 10 m/min), A_x will decrease if the depth of cut increases from 0.01 to 0.015 mm. If the depth of cut continues increasing, A_x will increase quickly. In the case the workpiece velocity was 15 m/min, if increasing the cutting depth, A_x will increase slowly.

-In all cases of the feed rate (2, 3, and 4 mm/stroke), A_x will decrease if the depth of cut increases from 0.01 to 0.015 mm. If the depth of cut continues increasing from 0.015 to 0.02 mm, A_x will increase.

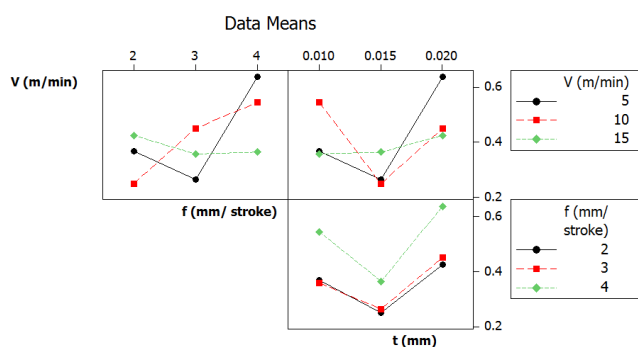


Figure 8. Interaction plot for A_x .

The interaction influence of input parameters on the system vibration amplitude in y direction (A_y) was described in Figure 9, the results from this figure showed that:

-In the case the workpiece velocity was 5 m/min: A_y will decrease quickly if the feed rate

increases from 2 to 3 mm/stroke. But if the feed rate continues increasing from 3 to 4 mm/stroke, A_y will increase quickly.

-If feed rate increases, A_y will increase in the case machining with the workpiece velocity of 10 m/min.

-In the case the workpiece velocity was 15 m/min: A_y will decrease slowly if the feed rate increases from 2 to 3 mm/stroke. But if the feed rate continues increasing from 3 to 4 mm/stroke, A_y will increase slowly.

-In both cases of the workpiece velocity (5 and 10 m/min), A_y will decrease quickly if the depth of cut increases from 0.01 to 0.015 mm. But, if the depth of cut continues increasing, A_y will increase quickly. In the case the workpiece velocity was 15 m/min, if the cutting depth increases, A_y will increase slowly.

-In all cases of the feed rate (2, 3, and 4 mm/stroke), A_y will decrease if the depth of cut increases from 0.01 to 0.015 mm. However, if the depth of cut continues increasing from 0.015 to 0.02 mm, A_y will increase.

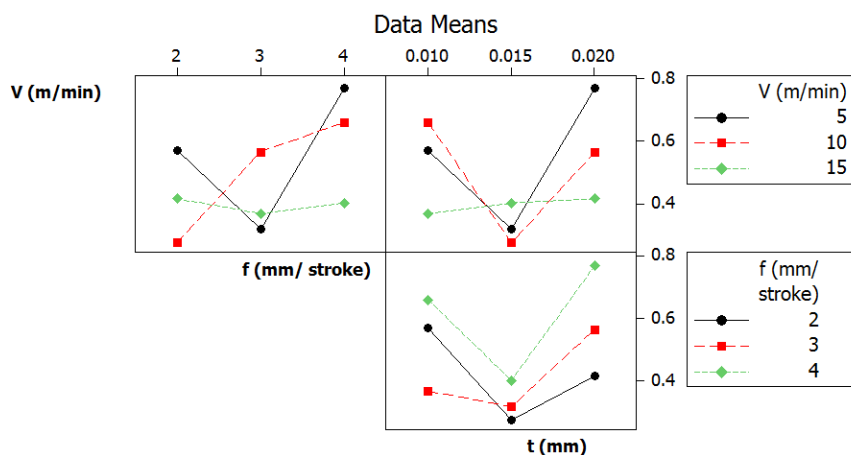


Figure 9. Interaction plot for A_y .

Figure 10 describes the interaction influence of input parameters on the system vibration amplitude in z direction (A_z), the results from this figure showed that:

-In two cases of the workpiece velocity (5 and 15 m/min): A_z will decrease if the feed rate increases from 2 to 3 mm/stroke. However, if the feed rate continues increasing from 3 to 4 mm/stroke, A_z will increase. If feed rate increases, A_z will increase in the case machining with the workpiece velocity of 10 m/min.

-In both cases of the workpiece velocity (5 and 10 m/min), if the depth of cut increases from 0.01 to 0.015 mm, A_z will decrease. But, if the depth of cut continues increasing from 0.015 to 0.02 mm, A_z will increase quickly.

-In the case the workpiece velocity was 5 m/min: if the depth of cut increases from 0.01 to 0.015 mm, A_z will increase slowly. But, if the depth of cut continues increasing from 0.015 to 0.02 mm, A_z will decrease slowly.

-In all cases of the feed rate (2, 3, and 4 mm/stroke), if the depth of cut increases from 0.01 to 0.015 mm, A_z will decrease. However, A_z will increase if the depth of cut continues increasing from 0.015 to 0.02 mm.

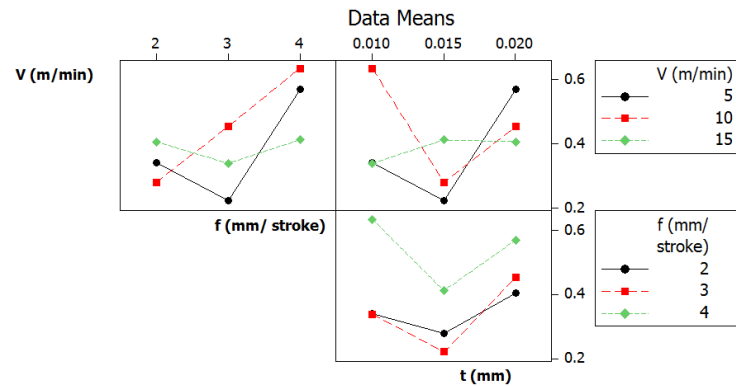


Figure 10. Interaction plot for Az.

From the above analyzed results, it seems that the degree and rule of input parameters on the machining surface roughness and system vibration component were quite complex. The interaction influence of these input parameters on the output parameters were more complex. To determine the input parameters with minimum values of surface roughness and system vibration components, and with maximum of material removal rate, the multi-objective optimization problem should be solved. In this case, five output parameters that were machining surface roughness and system vibration components (in X, Y, Z directions), and MRR were chosen as the objective functions of the multi-objective optimization problem. The contents of the multi-objective optimization problem were presented in next Section.

4. Multi-objective optimization using DEAR technique

4.1. DEAR method

The Data Envelopment Analysis Based Ranking (DEAR) method is one of the optimization method of machining processes. This is a simple method [29]. This method is more effective than several other methods [30–32]. However, up to now, it seems that there have not been any studies on surface grinding processes using CBN slotted grinding wheel in particular, and on applying DEAR method in optimizing the grinding process in general. In this study, the aim of the optimization process was the determination of the input parameters to obtain the minimum values of machining surface roughness and vibration amplitudes in X, Z, Y directions, and to obtain the maximum value of MRR. To solve the optimization problem, the DEAR technique that was used consisted of the steps as the follow [33–35]:

Step 1: Determine the weights (w) for each response for all experiments. Weight of response is the ratio between response at any trial to the summation of all responses.

Step 2: Transform the data of response into weighted data by multiplying the observed data with its own weight.

Step 3: Divide the data as smaller the better with smaller the better.

Step 4: Treat this value as multi response performance index (MRPI).

The MRPI was calculated by Eq 2.

$$MRPI = W_{Ra} * Ra + W_{Ax} * Ax + W_{Ay} * Ay + W_{Az} * Az + W_{MRR} * MRR \quad (2)$$

where the weights (w) for each response were calculated by Eqs 3–7.

$$W_{Ra} = \frac{Ra}{\sum Ra} \quad (3)$$

$$W_{Ax} = \frac{FAx}{\sum Ax} \quad (4)$$

$$W_{Fy} = \frac{Ay}{\sum Ay} \quad (5)$$

$$W_{Fz} = \frac{Az}{\sum Az} \quad (6)$$

$$W_{MRR} = \frac{1}{\sum \frac{1}{MRR}} \quad (7)$$

4.2. Multi-objective optimization of the grinding process of SUJ2 steel using CBN slotted wheel

From the experimental results in Table 5, the weight of each response and MRPI at each experiment were calculated by Eqs 2–7 and presented in Table 6.

Table 6. The response weight and MRPI at each experiment.

No.	Weight at each experiment					MRPI
	Ra	Ax	Ay	Az	MRR	
1	0.052113	0.100628	0.131037	0.093364	0.251768	2.0954
2	0.112964	0.071913	0.073203	0.060513	0.167845	1.8375
3	0.113644	0.17429	0.177097	0.15598	0.125884	3.1814
4	0.103547	0.06806	0.063134	0.076215	0.083923	1.6792
5	0.132313	0.123005	0.13023	0.124003	0.062942	2.6314
6	0.126584	0.148907	0.152051	0.173621	0.125884	3.0767
7	0.109708	0.116093	0.095783	0.111087	0.041961	2.2025
8	0.115684	0.097623	0.084885	0.092627	0.083923	2.0708
9	0.133446	0.099481	0.092581	0.112589	0.055948	2.2792

From the calculated values in Table 6, the MRPI values of all input parameters that were calculated by the total of MRPI of each parameter at the corresponding level and presented in Table 7.

Table 7. Total values of MRPI of the input parameters at the levels.

Parameters	Total values of MRPI at the levels			Max-Min
	1	2	3	
V	7.1144	7.3875	6.5525	0.8350
f	5.9771	6.5398	8.5373	2.5602
t	7.2429	5.7959	8.0153	2.2194

From the calculated results in Table 7, it showed that the optimal values as follow: the workpiece velocity at level 3 (15 m/min), feed rate at level 1 (4 mm/stroke), and depth of cut at level 2 (0.015 mm). These optimal parameters were used for testing experiments. The surface grinding processes of SUJ2 steel were performed using slotted CBN grinding wheel. The average values of output parameters were measured and calculated with the values as follow: surface roughness of 0.348 (μm), the A_x , A_y , A_z , and RMM of 0.2882 (μm), 0.3564 (μm), 0.3120 (μm), and 41.25 (mm^3/s), respectively. With these values of the output parameters, it shows that: Although R_a , A_x , A_y , A_z under testing experiments were not less than all the corresponding values of these parameters when compared with the experimental results in Table 5, the MRR was not also greater than all of the MRR values in this table. But clearly, the values R_a , A_x , A_y , A_z were all quite small, MRR was quite large (only smaller than MRR in the experiment 7 of Table 5). So, the values of the input parameters that were found in this study were the optimum values of the surface grinding process.

Besides, from the values of Table 7, the Max-Min value of the MPRI of the parameter with the greater value will have a larger influence on evaluation criteria in comparing to other parameters. In this study, The MRPI had the largest values of Max-Min were the feed rate (Max-Min = 2.5602). So, the feed rate was the most influence factor on the machining surface roughness, system vibration components, and MRR. The second factor that influence on the machining surface roughness, system vibration components, and MRR was depth of cut. The workpiece velocity had the negligible influence on the machining surface roughness, system vibration components, and MRR. These statements are consistent with the analyzed results in section 3. Thus, it can be confirmed that DEAR method has been successfully applied in determining the optimal value of the multi-objective problem in the surface grinding process of the SUJ2 steel using CBN slotted grinding wheel.

5. Conclusions

In this study, the CBN slotted grinding wheel was first used to machine the SUJ2 steel. Study has drawn the conclusions as following:

- The feed rate was the most influence factor on the machining surface roughness, system vibration components. The second factor that influence on the machining surface roughness and system vibration components was depth of cut. The workpiece velocity had the negligible influence on the machining surface roughness, system vibration components, and MRR.

- The degree and rule of input parameters on the machining surface roughness and system vibration components were quite complex.

- DEAR technique was also first applied to solve the multi-objective optimization problem of the surface grinding process of SUJ2 steel using the CBN slotted grinding wheel. The optimal values of input parameters were determined as following: The optimum values of input parameters were the

workpiece velocity of 15 m/min, the feed rate of 4 mm/stroke, and depth of cut of 0.015 mm. Using these optimal values, the average values of R_a , A_x , A_y , A_z , and MRR that were measured and calculated were 0.348 μm , 0.2882 μm , 0.3564 μm , 0.3120 μm , and 41.25 mm^3/s , respectively.

Taguchi method and DEAR technique can be applied to improve the quality of the machining surface, to reduce the system vibration components, and to increase the material removal rate. So, this method can be used to improve the quality and effectiveness of the surface grinding processes.

Acknowledgments

The authors thank Hanoi University of Industry (<https://www.hau.edu.vn/en>) for the support during the implementation of this study.

Conflict of interests

All authors declare no conflicts of interest in this paper.

References

1. Farsky J, Baksa T, Zetek M (2020) Grinding of maraging steel 1.2709 with SiC grinding wheels and effect of grinding conditions on the surface roughness and wear of the wheels. *Manuf Tech* 20: 18–22.
2. Marinescu LD, Rowe WB, Dimitrov B, et al. (2004) *Tribology of Abrasive Machining Processes*, 1 Ed., Elsevier.
3. Malkin S (1998) *Grinding Technology: Theory and Applications of Machining with Abrasives*, New York: Industrial Press.
4. Tu HX, Hong TT, Nga NTT, et al. (2019) Influence of dressing parameters on surface roughness of workpiece for grinding hardened 9XC tool steel. *IOP Conf Series: Materials Science and Engineering* 542: 012008.
5. Son NH, Trung DD, Nguyen NT (2020) Surface Roughness Prediction in Grinding Process of the SKD11 Steel by using Response Surface Method. *IOP Conf Series: Materials Science and Engineering* 758: 012029.
6. Haddad M, Zitoun R, Eym F, et al. (2016) The effect of rectification of composite materials on the mechanical behavior of long fiber composite materials. *AIMS Mater Sci* 3: 645–657.
7. Ronoh KN, Mwema FM, Akinlabi SA, et al. (2019) Effects of cooling conditions and grinding depth on sustainable surface grinding of Ti–6Al–4V: Taguchi approach. *AIMS Mater Sci* 6: 697–712.
8. Lee KW, Wong PK, Zhang JH (2000) Study on the grinding of advanced ceramics with slotted diamond wheels. *J Mater Process Technol* 100: 230–235.
9. Marinescu ID, Hitchiner MP, Uhlmann E, et al. (2006) *Handbook of Machining with Grinding Wheels*, New York: CRC Press.
10. Malkin S, Guo C (2008) *Theory and Applications of Machining with Abrasives*, 2 Eds., New York: Industrial Press.
11. Cao Y, Guan J, Li B, et al. (2013), Modeling and simulation of grinding surface topography considering wheel vibration. *Int J Adv Manuf Technol* 66: 937–945.
12. Malkin S (1984) Grinding of metals: theory and applications. *J Appl Metalwork* 3: 95–109.

13. Aini R, Rahnejat H, Gohar R (1990) A five degrees of freedom analysis of vibrations in precision spindles. *Int J Mach Tool Manu* 30: 1–18.
14. Liu T, Deng Z, Lv L, et al. (2020). Experimental analysis of process parameter effects on vibrations in the high-speed grinding of a camshaft. *Stroj Vestn-J Mech E* 66: 175–183.
15. Nguyen NT, Dung HT, Trung DD (2020) Multi-objective optimization when surface grinding the 3X13 steel by combining the general reduced gradient algorithm and harmonic mean method. *ASTESJ* 5: 395–400.
16. Li C, Li X, Wu Y, et al. (2019) Deformation mechanism and force modelling of the grinding of YAG single crystals. *Int J Mach Tools Manuf* 143: 23–37.
17. Li C, Wu Y, Li X, et al. (2019) Deformation characteristics and surface generation modelling of crack-free grinding of GGG single crystals. *J Mater Process Technol* 279: 116577.
18. Lee KW, Wong PK, Zhang JH (2000) Study on the grinding of advanced ceramics with slotted diamond wheels. *J Mater Process Technol* 100: 230–235.
19. Jin DX, Meng Z (2003) Research for discontinuous grinding wheel with multi-porous grooves. *Key Eng Mater* 259: 117–121.
20. Fan X, Miller M (2004) Force analysis for segmental grinding. *Proc of the ASPE Annual Meeting* 84: 87.
21. Handigund PB, Miller MH (2001) Abrasive wear and forces in grinding of silicon carbide. Available from: <https://pdfs.semanticscholar.org/9750/9eeb5d1820bfd6dd2dde60ff1b35d0198bc8.pdf>.
22. Phuong NT, Giang NTP, Dong NT (2017) Research on the affect of technologycal parameters on cutting temperature when machining use segmented grinding wheel. *IJECE* 8: 208–212.
23. Phuong NT, Nguyen GPT, Nguyen DT (2017) A research on the effect of cutting parameters on cutting force in flat grinding using segmentd grinding wheel. *Vietnam J Sci Technol* 55: 793–802.
24. Sinha MK, Setti D, Ghosh S, et al. (2016). An investigation on surface burn during grinding of Inconel 718. *J Manuf Process* 21: 124–133.
25. Shi Z, Malkin S (2006) Wear of electroplated CBN grinding wheels. *J Manuf Sci E-T Asme* 128: 1–9.
26. Yu T (2016) Material removal modeling and life expectancy of electroplated CBN grinding wheel and paired polishing. [PhD's thesis]. Iowa State University, Iowa.
27. Heat treatment guide. Available from: <https://steelnavigator.ovako.com/heat-treatment-guide/calculate/>.
28. About: 100Cr6. Available from: <https://steelnavigator.ovako.com/steel-grades/100cr6/>.
29. Manoj M, Jinu GR, Muthuramalingam T (2018) Multi response optimization of AWJM process Parameterson machining TiB2 particles reinforced Al7075 composite using Taguchi-DEAR methodology. *Silicon* 10: 2287–2293.
30. Muthuramalingam T, Vasanth S, Vinothkumar P, et al. (2018) Multi criteria decision making of abrasive flow oriented process parameters in abrasive water jet machining using Taguchi-DEAR methodology. *Silicon* 10: 2015–2021.
31. Muthuramalingam T, Loganathan GB, Atif A, et al. (2019) Multi response optimization on machining titanium alloy using Taguchi-DEAR analysis in abrasive water jet cutting. *SAE Tech Pap* 28: 1–5.

32. Huu NH, Muthuramalingam T (2020) Multi criteria decision making of vibration assisted EDM process parameters on machining silicon steel using Taguchi-DEAR methodology. *Silicon* 32: 1–7.
33. Reddy V, Sridhar C (2016) Multi response optimization of EDM of AA6082 material using Taguchi-DEAR method. *IJSTR* 7: 215–219.
34. Muthuramalingam T, Vasanth S, Rabik M, et al. (2016) Multi response optimization of EDM process parameters using assignments of weight method. *Int J Eng Res Technol* 4: 1–3.
35. Sandeep MJ, Manjunath PGC, Chate GR, et al. (2019) Multi response optimization of green sand moulding parameters using Taguchi-DEAR method. *Appl Mech Mater* 895: 1–7.



AIMS Press

© 2020 the Author(s), licensee AIMS Press. This is an open access article distributed under the terms of the Creative Commons Attribution License (<http://creativecommons.org/licenses/by/4.0>)